Hole Hopping Rates in Organic Semiconductors: A Second-Order Cumulant Approach

Hole Hopping Rates in Disordered Organic Semiconductors: a Second Order Cumulant Approach

Alessandro Landi,[†] Raffaele Borrelli,[‡] Amedeo Capobianco,[†] Amalia Velardo,[†] and Andrea Peluso[*,†]

[†]*Dipartimento di Chimica e Biologia Adolfo Zambelli, Università di Salerno, Via Giovanni Paolo II, I-84084 Fisciano (SA), Italy*

[‡]*Department of Agricultural, Forestry and Food Science, University of Torino, I-10195 Grugliasco, Italy*

E-mail: apeluso@unisa.it

Abstract

Second-order cumulant expansion of the time dependent reduced density matrix has been employed to evaluate hole hopping rates in pentacene, tetracene, picene, and rubrene homodimers. The cumulant expansion is a full quantum mechanical approach, which allows to use in computations the whole set of nuclear coordinates of the system, including both the effects of the equilibrium position displacements and of normal mode mixing upon hole transfer. The time dependent populations predicted by cumulant approach are in good agreement with those obtained by numerical solution of time dependent Schrödinger equation, even for ultrafast processes, where the Fermi Golden Rule fails. Field effect mobility in disordered systems where the establishment of a hopping regime is plausible are in line with experimental findings.

Introduction

Organic π-conjugated single molecules and polymers have revealed to be extremely useful building blocks for developing efficient optoelectronic materials. The impressive progresses obtained in the fields of organic light emitting diodes (OLEDs) and solar energy conversion have allowed to achieve efficiencies high enough to reach the market, with still high expectations of further improvements.[1,2] Organic field-effect transistors (OFETs) are also of great technological interest for the fabrication of low cost, flexible, and large area logic circuitry.[3–13] In that context, theoretical approaches for determining rate constants of elementary processes – hole transfer (HT), electron transfer (ET), charge recombination – taking place in those devices is certainly of help for designing new molecules with improved performances and for understanding the underlying physico-chemical mechanisms. Up to now, rate constants for charge transfer and charge recombination processes have been evaluated either by Marcus' semiclassical approach or by Fermi Golden Rule (FGR). While the former does not account for tunneling effects, the latter, a full quantum mechanical approach at the first order of time dependent perturbation theory, has limitations in very short or long transition times. Herein, we use the second order cumulant (SOC) expansion of the reduced density matrix for evaluating hole hopping rates in homodimers of organic molecules mostly employed in organic semiconductors. Similarly to Fermi Golden Rule (FGR), the SOC expansion of the time dependent reduced density matrix is a full quantum mechanical approach, able to handle the whole set of nuclear coordinates, which should provide a significant improvement with respect to FGR approach, at least for ultrafast hole hopping processes, inasmuch as it does not require the use of integral representation of the Dirac delta function. By using a standard Montecarlo approach, we show that SOC rates provide reliable 3D averaged hole mobilities, comparable with those observed for disordered systems, in which the establishment of a hopping regime is plausible, and exhibiting temperature dependencies in line with the experimental results.

Hopping rates

Marcus' theory

Semiclassical Marcus' theory[14,15] has been widely used for computing hole hopping rates in organic materials.[16,17] For hopping between two equal molecules the net ΔG change is zero and the charge transfer rate k is:

$$k = \frac{|V|^2}{\hbar}\sqrt{\frac{\pi}{\lambda k_{\mathrm{B}} T}}\exp\left[-\frac{\lambda}{4k_B T}\right] \tag{1}$$

where V is the electronic coupling parameter and λ is the reorganization energy, which consists of an intramolecular and an intermolecular contribution, due to equilibrium position changes of the system and of the surrounding medium upon hole transfer. Computations carried out by using a QM/MM approach with a polarizable force field for naphthalene in its molecular crystal structure showed that the intermolecular reorganization energy is small, of the order of a few meV;[18] further studies for acenes yield intermolecular reorganization energies typically lower than 0.2 kcal/mol,[17] much smaller than the intramolecular one.

Fermi's golden rule

Fermi's Golden rule expression of the rate of an electronic transition between two electronic states $|i\rangle$ and $|f\rangle$ is:

$$k = \frac{2\pi}{\hbar}|V|^2 F(\Delta E, T), \tag{2}$$

where V is the electronic coupling element, which has been assumed in deriving eq.n 2 to be independent of vibrational coordinates, ΔE is the electronic energy difference between the initial and final states, T is temperature, and $F(\Delta E, T)$ is the Franck-Condon weighted

density of states given by:

$$F(\Delta E, T) = \frac{1}{Z}\sum_{v_i, v_f} \mathrm{e}^{-\beta E_{v_i}} |\langle v_i | v_f \rangle|^2 \delta\big(E_{v_f} - E_{v_i} - \Delta E\big), \tag{3}$$

where $\langle v_i | v_f \rangle$ is the Franck-Condon integral, Z is the vibrational partition function of the initial electronic state, $\beta = 1/k_{\mathrm{B}}T$, and the sum runs over all vibrational states of $|i\rangle$ and $|f\rangle$.

The evaluation of $F(\Delta E, T)$ by the infinite summations of eq.n 3 poses problems which can be avoided by using the generating function (GF) approach developed in the fifties by Lax and Kubo,[19,20] which makes use of the integral representation of the Dirac delta function. By using the harmonic approximation and Duschinsky's normal mode transformation:

$$\mathbf{Q}_i = \mathbf{J}\mathbf{Q}_f + \mathbf{K},$$

$F(\Delta E, T)$ can be evaluated from the normal modes ($\mathbf{Q}$) and vibrational frequencies of the initial and final states, including the whole sets of nuclear coordinates in computations.[21–25] Endoergonic transitions, possibly due to significant reorganization energies of the environment, can be treated by resorting to the principle of detailed balance,[26–28] according to which the rate of the endoergonic $|i\rangle \rightarrow |f\rangle$ process is obtained from that of the reverse exoergonic process by the relation:

$$k_{if} = k_{fi} \exp[-\Delta E_{if}/k_B T],$$

where k_{fi} is evaluated at ΔE_{fi}.

Second order cumulant approximation

The rate expression of eqns 2 and 3 holds true in the limit of sufficiently long transition times and therefore it must be used with caution for ultrafast processes. A possible way out is provided by the second-order cumulant expansion of the time dependent reduced density

matrix. The cumulant expansion is a well known technique,[29–32] but rather few applications to realistic microscopic Hamiltonians have appeared in the literature.[33–35] In the case of interest here, two electronic states $|i\rangle$ and $|f\rangle$, with a constant perturbation:

$$\mathcal{H} = |i\rangle\,\mathcal{H}_i\langle i| + |f\rangle\,\mathcal{H}_f\langle f| + |i\rangle\,V\langle f| + c.c. = \mathcal{H}^0 + V, \tag{4}$$

where $\mathcal{H}_i$ and $\mathcal{H}_f$ are the vibrational Hamiltonian of the electronic states $|i\rangle$ and $|f\rangle$ respectively, the second order cumulant approximation of the population of the initial state is given by:[30,35]

$$P_i(t) = \exp(K_2(t))$$

with:

$$K_2(t) = -2\hbar^{-2}\mathrm{Re}\mathrm{Tr}\int_0^t \mathrm{d}\tau_1 \int_0^{\tau_1} \langle i|[V_I(\tau_2),[V_I(\tau_2),\rho(0)]]\,|i\rangle\,\mathrm{d}\tau_2. \tag{5}$$

where the trace is evaluated over the whole set of the vibrational states of the initial state, and $V_I(s)$ is the interaction representation of the coupling potential V.

By using for $\rho(0)$ the thermal equilibrium distribution, eq.n 5 becomes:

$$K_2(t) = -2\hbar^{-2}Z^{-1}\mathrm{Re}\int_0^t \mathrm{d}\tau_1 \int_0^{\tau_1} \mathrm{Tr}(\mathrm{e}^{\mathrm{i}\mathcal{H}_i(\tau_2+\mathrm{i}\beta)}V_{if}\mathrm{e}^{-\mathrm{i}\mathcal{H}_f\tau_2}V_{fi})\mathrm{d}\tau_2 \tag{6}$$

If the initial state is prepared in a non equilibrium distribution, which for the case of fast hole transfer could be the thermally equilibrated ground state of the neutral molecule which istantaneously releases an electron, the initial density for hole transfer is given by:

$$\rho(0) = Z_N^{-1}\,|i\rangle\,\mathrm{e}^{-\beta\mathcal{H}_N}\langle i|.$$

$\mathcal{H}_N$ being the vibrational Hamiltonian of the neutral molecule and Z_N its corresponding

vibrational partition function, and the second order cumulant average becomes:

$$K_2(t) = -\hbar^{-2} Z_N^{-1} \mathrm{Re} \int_0^t \int_0^t \mathrm{Tr}(\mathrm{e}^{-\beta \mathcal{H}_N} \mathrm{e}^{\mathrm{i}\mathcal{H}_i^{\circ} \tau_2} V_{if} \mathrm{e}^{-\mathrm{i}\mathcal{H}_f(\tau_2 - \tau_1)} V_{fi} \mathrm{e}^{-\mathrm{i}\mathcal{H}_i \tau_1}) \mathrm{d}\tau_1 \mathrm{d}\tau_2. \quad (7)$$

The finite integration time in equations 6 and 7 allows to explicitly take into account the effect of a non-zero correlation time of the second order autocorrelation function:[32] $\left\langle i \right| [V(\tau_1), [V(\tau_2), \rho(0)]] \left| i \right\rangle$. As we shall see below this effect is important when the number of vibrational modes coupled to the electronic degrees of freedom is small and their reorganization energy is not too large.

Computational details

Equilibrium geometries, normal modes, and vibrational frequencies of pentacene, picene, rubrene, and tetracene in their neutral and cationic forms were obtained at the DFT level using the B3LYP functional with the 6-31+G(d,p) basis set, which has been proved to yield sufficiently accurate results.[36] Dielectric effects have been estimated by using the polarizable continuum model (PCM).[37] According to previous works, we have assumed $\epsilon = 4$ as the average value for the dielectric constants of the bulk materials.[38] The G09 package has been used for electronic wavefunction computations.[39] Photoelectron spectra and Franck-Condon weighted densities of states have been computed by using a development version of the MolFC package.[?] Intermolecular reorganization energies have been neglected. The curvilinear coordinate representation of the normal modes has been adopted to prevent that large displacements of an angular coordinate could reflect into large shifts of the equilibrium positions of the involved bond distances. That is unavoidable in rectilinear Cartesian coordinates and requires the use of high order anharmonic potentials for its correction.[24,41–45] The evaluation of the time-dependent rates $K_2(t)$ of eqn.s 6 and 7 is based on the coordinate representation of the reduced density matrix; the resulting multidimensional Gaussian type integrals have been evaluated analytically.[46] The numerical solution of

the time-dependent Schrödinger equation has been carried out by using an orthogonalised Krylov subspace method;[47,48] more details are provided in the Supporting Information.

Rate constants

We will apply Marcus, FGR and SOC approaches for determining hole hopping rates in homodimers of pentacene, rubrene, picene, and tetracene, organic molecules of interest in the field of organic field effect transistors.

The elementary hole transfer reactions is modeled as the redox process:

$$X_1^+ + X_2 \rightarrow X_1 + X_2^+ \tag{8}$$

taking place into a dimer formed by two adjacent molecules, immersed in a continuum dielectric medium.

Computed normal mode equilibrium position displacements for the hole injection half reaction and their contributions (harmonic approximation) to the total reorganization energies are reported in Table 1, together with the total electronic intramolecular reorganization energies computed at PCM/B3LYP level, using an effective dielectric constant ϵ=4. The effect of the dielectric constant is almost insignificant on both equilibrium position displacements and reorganization energies, as shown by the results obtained in the gas-phase, reported in the Supporting Information.

From the components of the **K** vectors of Table 1, the photoelectron spectra of the four molecules have been computed and compared with the available experimental results.[51–53] The results are reported in the Fig. 1; the agreement between computed and experimental spectra is extremely good, testifying about the reliability of the adopted computational approach.

Slight discrepancies between computed and measured spectra have been found only for

Table 1: Wavenumbers (ω, cm^{-1}), intramolecular reorganization energies (E_r, cm^{-1}), and equilibrium position displacements (**K**, Å uma$^{-1/2}$) of the most displaced normal modes of pentacene/pentacene$^+$ (P/P$^+$), picene/picene$^+$(PC/PC$^+$), rubrene/rubrene$^+$ (R/R$^+$) and tetracene/tetracene$^+$ (T/T$^+$) redox pairs. All data refer to hole injection X $\rightarrow$ X$^+$

P/P$^+$			PC/PC$^+$			R/R$^+$			T/T$^+$		
ω	E_r^a	**K**	ω	E_r^a	**K**	ω	E_r^a	**K**	ω	E_r^a	**K**
263	9.2	−0.36	32	30.1	−1.0	24	72.6	2.3	317	9.3	−0.24
797	2.7	-8.2×10^{-2}	259	45.2	−0.59	68	10.6	0.57	761	4.3	0.11
1023	6.3	−0.11	425	9.5	0.21	89	28.9	0.86	1186	23.1	−0.20
1186	12.8	−0.15	593	70.2	−0.49	214	14.2	0.36	1232	61.1	−0.31
1213	54.2	−0.29	1390	216.7	−0.56	252	8.0	0.25	1420	24.0	−0.18
1421	105.6	−0.43	1654	142.5	0.42	995	20.4	−0.20	1435	141.9	−0.44
1564	130.5	0.41	1665	136.1	−0.41	1340	126.2	−0.43	1652	112.0	−0.38
						1583	107.8	0.37			
$E_\mathrm{r,tot}^b$	382			736			608			448	

[a] Computed by harmonic approximation from **K** components; [b] from electronic computations.

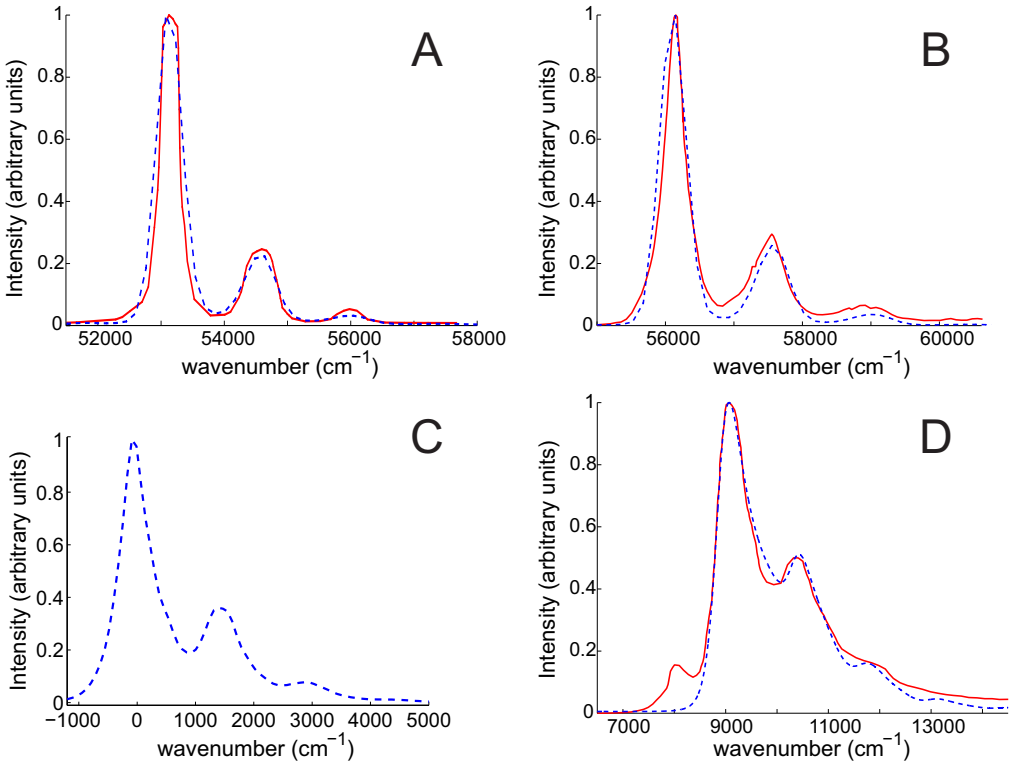

Figure 1: Experimental (red full line) and computed (blu dashed line) photoelectron spectrum of: pentacene at $T = 505$ K (A); tetracene at $T = 480$ K (B); picene at $T = 468$ K (C); rubrene at $T = 140$ (D). The experimental spectra have been digitized from ref.s 51–53, respectively. The experimental spectrum of picene is not shown because it exhibits two overlapping electronic transitions, a complication not considered here.

rubrene and only in the spectral region where hot transitions occur. A more reliable treatment of that spectral region would require use of anharmonic potentials,[43,45] which would be unmanageable in the all mode computations of hole transfer rates, therefore we have not afforded this task. For picene the experimental spectrum from ref. 51 has not been shown because it exhibits two overlapping electronic transitions and therefore it can not be compared to the simulated spectrum, in which only the first transition has been considered.

Computed Franck-Condon weighted densities of states ($F(\Delta E, T)$) for hole hopping in homodimers are reported in Figure 2 as a function of ΔE. For the two acenes, $F(\Delta E, T)$ is a narrow function of ΔE, strongly peaked around $\Delta E = 0$ with a total width of about 3000 cm^{-1}. On the contrary, for both rubrene and picene dimers $F(\Delta E, T)$ is much broader, with a total width of more than 6000 cm^{-1}. Those significant differences are due to the fact that rubrene and picene possess displaced normal modes at energies well below the thermal energy at $T = 298$ K, whereas pentacene and tetracene do not, see Table 1.

Marcus and FGR hole hopping rates evaluated at $T = 298$ K are reported in Table 2, for V=1cm^{-1}. FGR rates have been obtained either at $\Delta E = 0$, as usual in the literature, or by averaging $F(\Delta E, T)$ over a range of 400 cm^{-1} around $\Delta E = 0$.

Table 2: Kinetic rate constants ($\times 10^8$ s^{-1}) for hole transfer in homodimers for V=1cm^{-1}and T=298 K. Averaged SOC rate constants refer to the hole hopping path with the largest V.

	Marcus	FGR$^a_{\rm av}$	FGR	SOC$^b_{\rm eq}$	SOC$^c_{\rm neq}$
Pentacene	3.3	12.1	25.1	3.4	3.1
Picene	1.0	2.3	2.5	2.4	3.2
Rubrene	1.6	1.5	1.9	1.7	2.6
Tetracene	2.6	12.3	27.5	3.5	3.4

[a] From averaged Franck-Condon weighted density of states; [b] initial state from the equilibrium thermal distribution of the cationic state; [c] initial state from the equilibrium thermal distribution of the neutral state.

The transfer integrals for the intermolecular arrangements corresponding to the fastest hole paths,[49,50] see figure 3, together with the normalized ($V = 1$ cm^{-1}) rate constants of table 2 yield for pentacene and tetracene hopping times of the order of a few femtoseconds.

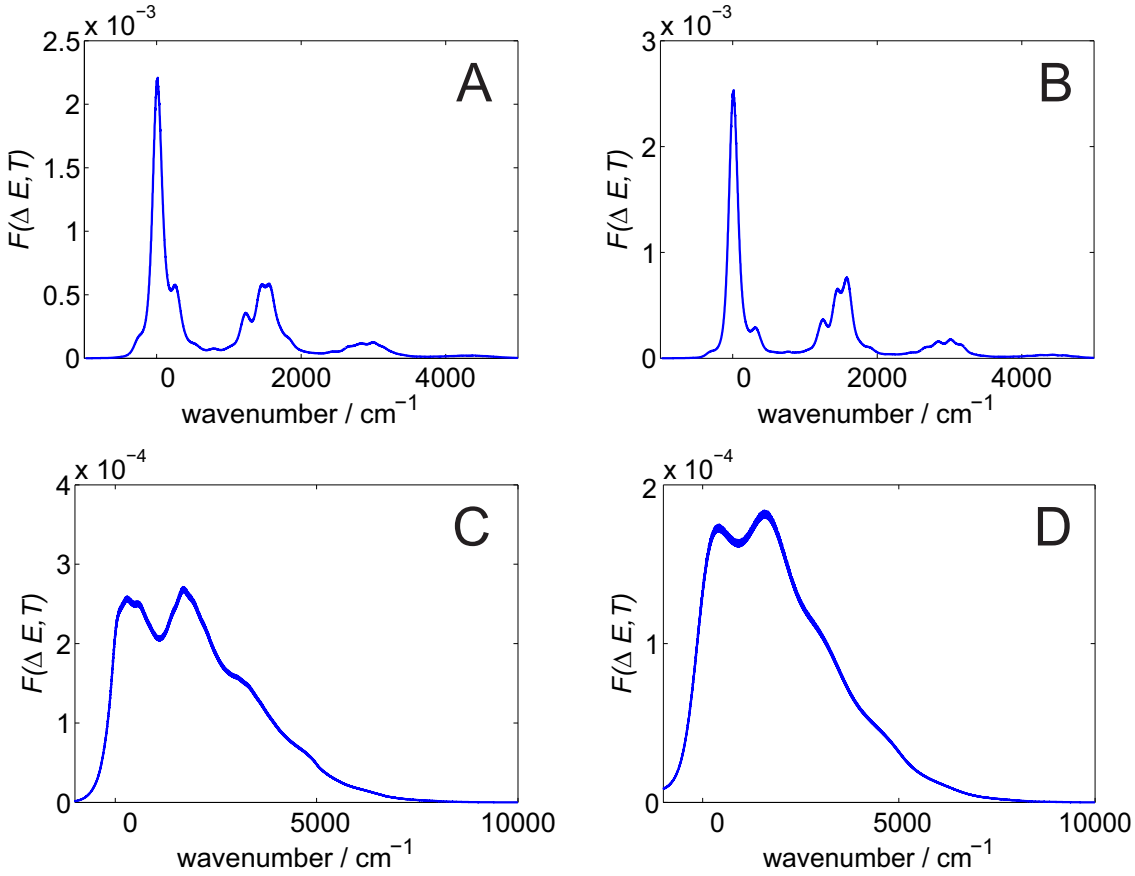

1

Figure 2: Computed densities of states for hole hopping in pentacene (A), tetracene (B), picene (C), and rubrene (D). $T = 298$ K; all mode calculation.

For such ultrafast transitions, the integral representation of Dirac delta function used in the computation of $F(\Delta E, T)$, eq.n 3, could be inappropriate and could lead to significant overestimation of the transition rates obtained by FGR approach. We have checked that by evaluating time dependent populations $P(t)$ for hole transfer in a dimer using the second order cumulant approach, setting in all the cases $\Delta E = 0$, and adopting as initial state the hole fully localized on a molecular unit, either in the equilibrium thermal distribution of the cationic state or in the equilibrium distribution of the neutral state, the latter choice being better suited when hole transfer is fast enough to compete with vibrational relaxation to the thermal equilibrium distribution. The results are reported in Figure 4 for pentacene and tetracene, where time decay probabilities of the initial state predicted by the SOC approach are compared with the monoexponential decay of FGR.

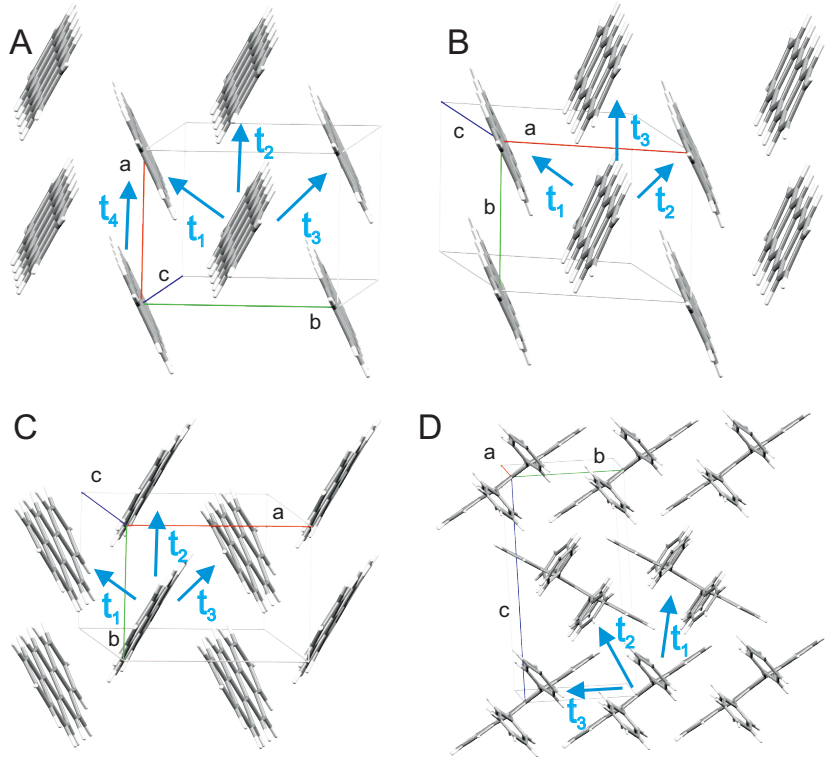

Figure 3: Hole hopping paths in: pentacene (A), tetracene (B), picene (C), and rubrene (D) crystal structures. The computed electronic coupling elements (meV) are: pentacene $t_1 = 75$, $t_2 = 20$, $t_3 = 32$, $t_4 = 6$; rubrene $t_1 = 19$, $t_2 = 19$, $t_3 = 89$; picene $t_1 = 66$, $t_2 = 70$, $t_3 = 54$; tetracene $t_1 = 17$, $t_2 = 70$, $t_3 = 1$.[49,50]

Figure 4 shows that the SOC approximation yields significantly longer transition times

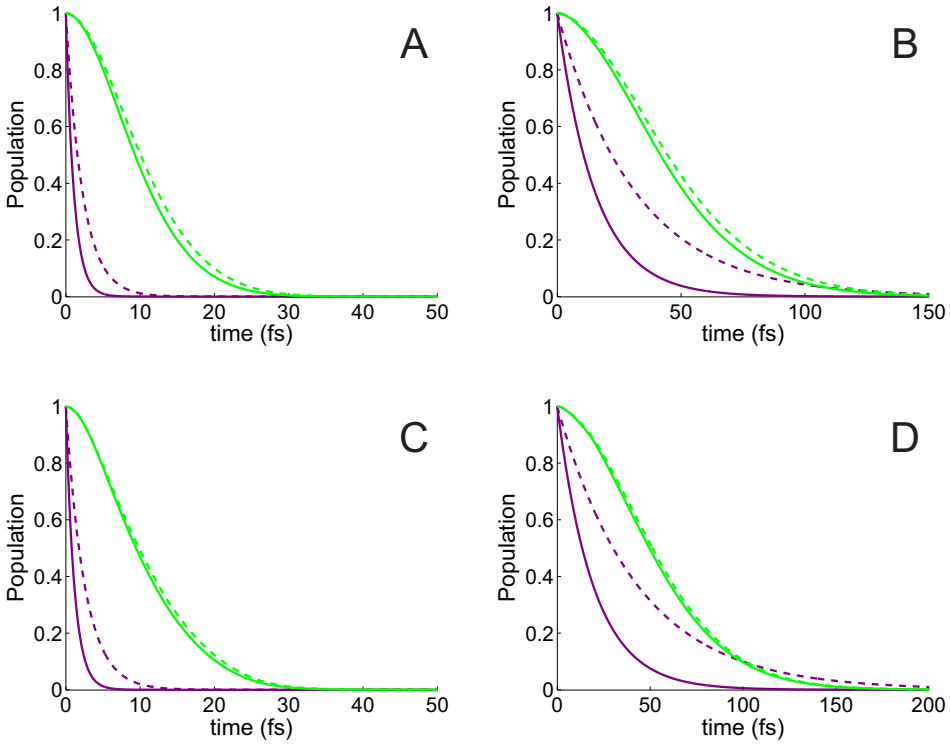

Figure 4: Time decay probabilities predicted by FGR and SOC approaches for hole hopping in pentacene and tetracene dimers. A: pentacene channel 1; B: pentacene channel 2; C: tetracene channel 2; D: tetracene channel 1. Purple full line: FGR at $\Delta E = 0$; purple dashed line: FGR averaged over 400 cm^{-1} around $\Delta E = 0$; green full line: equilibrium second order cumulant; green dashed line: non-equilibrium second order cumulant. $T = 298$ K; all mode calculation.

than FGR one, especially for fast decay rates. For channel 1 of pentacene and channel 2 of tetracene, FGR predicts that the initial state completely decays within 5 fs, whereas SOC approach yields a decay time of about 30 fs. Slightly longer decay times are predicted by FGR when the energy averaged Franck-Condon weighted density of states is used, but decay times are still very short. For pentacene and tetracene, SOC decay rates are roughly independent of the initial population, a consequence of the fact that all the displaced modes of the two redox pairs fall at high wavenumbers and that $F(\Delta E, T)$ is strongly peaked at $\Delta E = 0$. Both factors concur in making the thermal equilibrium distributions of both the neutral and the cationic states nearly coincident with the ground state.

Those results show that in pentacene and tetracene hole transfer involves a few vibronic states and FGR is therefore inadequate to treat them. Rubrene and picene behave differently, inasmuch as they exhibit low frequency vibrational modes whose equilibrium positions are displaced upon hole transfer. As shown in Figure 6, the decay rates predicted by FGR and SOC approaches are very similar; FGR still predicts slightly faster rates for picene, which possesses only one low frequency displaced mode, and for the fastest hole channel of rubrene, whereas for the slowest hole paths of rubrene, channel 1 and 2 of Figure 3, it provides decay rates which are indistinguishable from those obtained by SOC computations. Furthermore, in both picene and rubrene SOC decay rates depend on the initial population: the equilibrium thermal populations of the neutral state always provide faster rates than those of the cationic one.

In order to provide an easier way of comparison among the different approaches, coarse grained time averages of the SOC rate constants, obtained by a monoexponential fit of the SOC time dependent populations at T=298 K and referring only to the fastest paths, have also been reported in Table 2. The temperature dependence of the averaged SOC rate constants is shown in figure **??**, together with the temperature dependence obtained by Marcus and FGR approaches. While the latter ones yield rates which significantly depend on temperature, exhibiting opposite T dependence, see figure **??**, the averaged SOC rate constants

have a much slight temperature dependence. In the case of pentacene the hopping rates is independent of T, as it would be expected from the computed normal modes equilibrium position displacements of table 1. Vice versa, FGR yields rate constants which significantly decrease as T increase, which is another artifact of the already discussed inapplicability of FGR to those ultrafast processes. In the case of rubrene FGR and SOC approaches yield very similar results in the region 100-200 K. For higher values of T FGR predicts a smooth decrease of k, not found in the SOC results, possibly because of the adopted average procedure. Noteworthy, although Marcus and SOC approaches yield comparable results at room temperature, the predicted T dependence is very different, posing limits to the use of the semiclassical approach for studying the temperature-dependence of hole transport in organic materials.

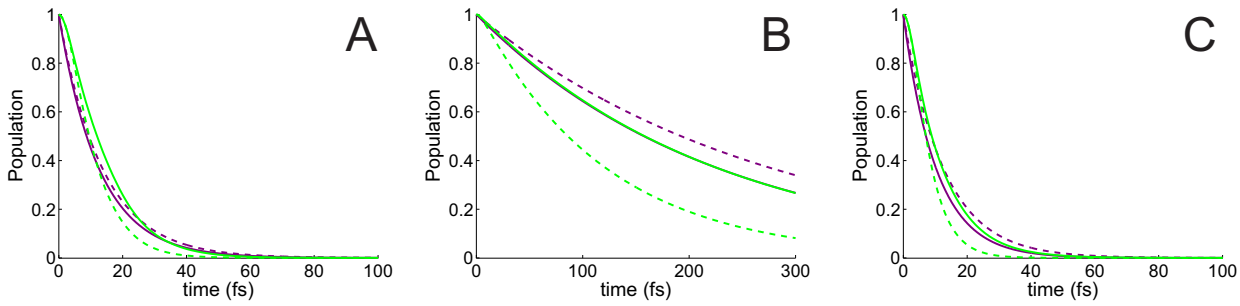

Figure 5: Time decay probabilities for hole hopping in picene and in rubrene. A: picene channel 2; B: rubrene channel 1; C: rubrene channel 3. Purple full line: FGR at $\Delta E = 0$; purple dashed line: FGR averaged over 400 cm^{-1} around $\Delta E = 0$; green full line: equilibrium second order cumulant; green dashed line: non-equilibrium second order cumulant. $T = 298$ K; all mode calculation.

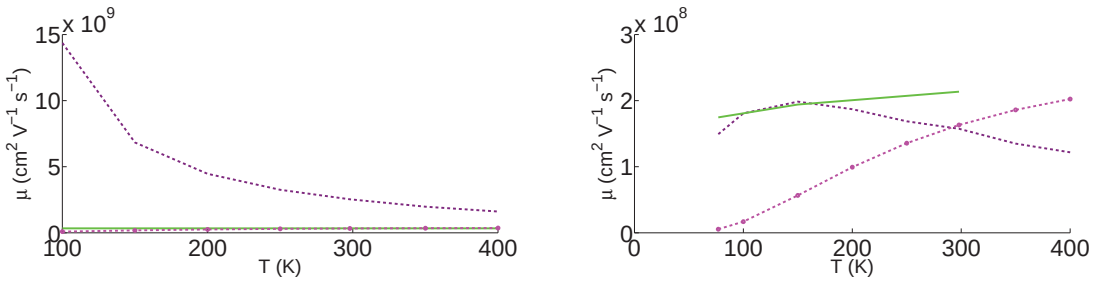

Figure 6: Hole hopping rate constants in homodimers at different temperatures by FGR (black dashed line), Marcus (purple dashed line), and equilibrium second order cumulant (green line).

For better assessing the reliability of the SOC approach, we have also computed decay

rates by the numerical solution of the time dependent Schrödinger equation (TDSE) with the Hamiltonian of eq.n 4. In those computations, in order to limit the exponential growth of the computational load with increasing basis sets,[54] only the subsets of displaced modes reported in Table 1 have been considered, which, at any rate, account for more than 80% of the total reorganization energies for all the molecular units. The size of the basis set and of the active space has been chosen in such a way to have converged results for the time interval considered here; it was selected using a recently developed methodology for an efficient partitioning of the Hilbert space,[55] described in the Supporting Information.

For pentacene and tetracene only the ground vibrational state, either of the cationic or of the neutral species, has been populated at $t = 0$, whereas for picene and rubrene, which exhibits several low frequency displaced modes, hole dynamics at room temperature is described using an approach based on the thermo field dynamics theory, a formulation which allows to treat temperature effects in the Hilbert space.[46] For rubrene and picene, only the equilibrium thermal distribution corresponding to the hole fully localized on a molecular unit has been considered. The results are reported in figure 7 for the fastest hole paths of the four molecular materials. The time decay of the initial state predicted by numerical solution of TDSE and SOC expansion of the reduced density matrix agree very well each other at shorter times, up to TDSE solutions begin to oscillate between the initial and final state, which, of course, is prevented in the SOC approach.[35] Thus, SOC expansion appears to provide a computationally economical and reliable way for estimating hole transfer rates including the whole set of intramolecular vibrational coordinates. Generalization to include phonon or intermolecular vibrations should not pose any computational problem if the nature of those modes and their coupling elements were known.

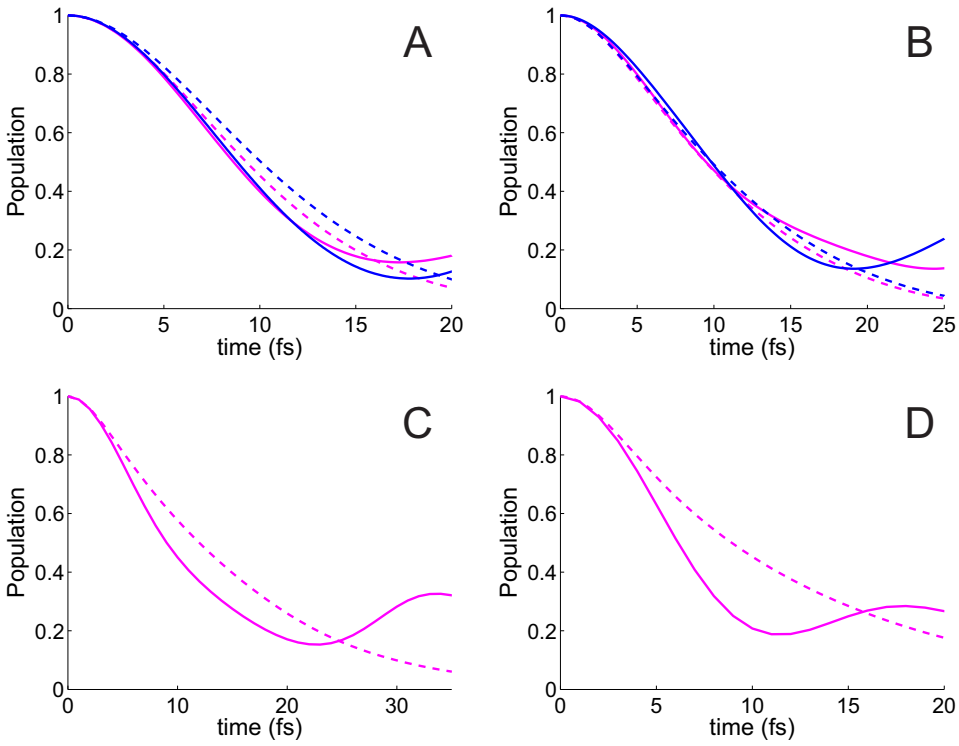

Figure 7: Comparison between time decay probabilities for hole hopping in dimers predicted by the numerical solution of the time dependent Schrödinger equation, full line, and from second order cumulant expansion of the reduced density matrix, dotted line. Initial state: equilibrium thermal population of the cationic state, magenta; equilibrium thermal population of the neutral state, blue. I: Pentacene channel 1; II: Tetracene channel 2; III: picene channel 2; IV: rubrene channel 3.

Hole mobilities in disordered systems

The mechanism of hole transport in organic semiconductors is still a matter of intense debate. Neither the hopping nor the band-like mechanism appears to be adequate models for treating charge transport in those materials.[56–61] From the one hand, highly purified crystals of pentacene and rubrene exhibit high mobilities with a temperature dependence which would point toward a band-like mechanism.[62] From the other hand, there is experimental evidence showing that the mean free paths of charge in organic materials is close to the intermolecular distances, which somewhat conforms to the hopping mechanism.[64,65] Theoretical calculations based on quantum coherent models yield mobility two order of magnitude higher than experimental ones,[21,63] evidencing that thermal disorder and the interactions of the charge carrier with the intermolecular vibrations have to play an important role.[56] Herein, we will limit to

consider highly disordered systems, where grain boundaries and interfacial disorder significantly limit hole transport, making plausible a hopping mechanism. 2D averaged mobilities have been computed by using the approach of Shuai et al.,[21] in which charge mobilities are obtained by Einstein' relation:

$$\mu = \frac{eD}{k_B T},$$

and the isotropic diffusion constants are obtained by the random walk simulations as described in ref. 21. In short, we make the plausible assumption that even in highly disordered systems the hole has always a possible neighbor site for hopping. The hop probabilities for the i-th path of figure **??** (p_i) is determined by the rate constants for hole transfer in homodimers obtained by the SOC approach:

$$p_i = \frac{k_i}{\sum_i k_i},$$

and the hopping direction during the random walk simulation is determined by generating a random number ranging from 0 and 1. The hopping time is $1/k_i$ and the hopping distances are taken as the molecular center-center distance along each path. Following previous work,[21] the time of each simulation is set to 10 μs, the squared displacements are saved each 100 ns, and averaged over several hundreds simulations, in order to obtain a linear relationship between the diffusion time and the square of the diffusion distance. The statistical error on mobilities is computed by performing new sets of similar simulations and evaluating for each set new mobilities; a few hundreds of those simulations are taken randomly from those previously computed. The error is then obtained as $\mu_{max} - \mu_{min})/2$. Details about the results of the random walk simulations are reported in the Supporting Information. 2D averaged mobilities have been computed only for rubrene and pentacene, the most interesting materials for technological applications; the results are reported in figure **??** for T= 77,150, and 298 K. Mobilities for pentacene range from 2.3±0.3 at T=77 K to 0.6±0.08 at T=298 K, which compare reasonably well with the available experimental results, reporting for pentacene thin

films mobilities varying from 0.2 up to 1.5 at room temperature.[72,73] Experimental results have shown that the macroscopic transport properties of thermally evaporated thin films of pentacene exhibit significant variations even in sample grown under nominally identical conditions: for the samples characterized by the highest mobilities a nearly temperature-independent regime has been observed, whereas for samples with significant lower mobilities a thermally activated hopping transport seems to be operative.[73] Our results indicate that, under the assumptions that disorder only affect the direction of the charge transport in the solid material, pentacene mobilities follow a simple 1/T temperature dependence, due to the fact that hopping rates do not appreciably depend on temperature.

Conclusions

The second order cumulant approach appears to provide a computationally economical and reliable way for estimating hole transfer rates, including their temperature dependence. Since it is based on a finite integration time, it allows to explicitly take into account the effect of a non-zero correlation time of the second order autocorrelation function,[32] which can be important when the number of vibrational modes coupled to the electronic degrees of freedom is small and their reorganization energy is not too large, the case where FGR fails.
Marcus' semiclassical approach can provide qualitatively correct values of transition rates, but it is unable to provide reliable temperature dependencies when tunneling effects predominate.

Acknowledgement

The financial supports of the University of Salerno and of the European Community (PON Relight project) are gratefully acknowledged. Authors acknowledge the CINECA awards HP10CYW18T and HP10CB456N under the ISCRA initiative for the availability of high-performance computing resources.

Supporting Information Available

Orthogonalised Krilov subspace method used in TDSE simulations is described. Quantum dynamics simulation not shown in the article (Figure S1-S3). Equilibrium position displacements and reorganization energies in the gas-phase for the four molecules studied (Table S1).

This material is available free of charge via the Internet at `http://pubs.acs.org/`.

References

(1) Wu, J.; Lan, Z.; Lin, J.; Huang, M.; Huang, Y.; Fan, L.; Luo, G. Electrolytes in Dye-Sensitized Solar Cells. *Chem. Rev.* **2015**, *115*, 2136–2173.

(2) Scholz, S.; Kondakov, D.; Lüssem, B.; Leo, K. Degradation Mechanisms and Reactions in Organic Light-Emitting Devices. *Chem. Rev.* **2015**, *115*, 8449–8503.

(3) Arias, A. C.; MacKenzie, J. D.; McCulloch, I.; Rivnay, J.; Salleo, A. Materials and Applications for Large Area Electronics: Solution-Based Approaches. *Chem. Rev.* **2010**, *110*, 3–24.

(4) Yan, H.; Chen, Z.; Zheng, Y.; Newman, C.; Quinn, J. R.; Dotz, F.; Kastler, M.; Facchetti, A. A High-Mobility Electron-Transporting Polymer for Printed Transistors. *Nature* **2009**, *457*, 679–686.

(5) Tang, M. L.; Mannsfeld, S. C. B.; Sun, Y.-S.; Becerril, H. A.; Bao, Z. Pentaceno[2,3-b]thiophene, a Hexacene Analogue for Organic Thin Film Transistors. *J. Am. Chem. Soc.* **2009**, *131*, 882–883.

(6) Baeg, K.-J.; Noh, Y.-Y.; Sirringhaus, H.; Kim, D.-Y. Controllable Shifts in Threshold Voltage of Top-Gate Polymer Field-Effect Transistors for Applications in Organic Nano Floating Gate Memory. *Adv. Funct. Mat.* **2010**, *20*, 224–230.

(7) Tang, Q.; Jiang, L.; Tong, Y.; Li, H.; Liu, Y.; Wang, Z.; Hu, W.; Liu, Y.; Zhu, D. Micrometer- and Nanometer-Sized Organic Single-Crystalline Transistors. *Adv. Mat.* **2008**, *20*, 2947–2951.

(8) Yamada, H.; Okujima, T.; Ono, N. Organic Semiconductors Based on Small Molecules With Thermally or Photochemically Removable Groups. *Chem. Commun.* **2008**, 2957–2974.

(9) Toffanin, S.; Capelli, R.; Hwu, T.-Y.; Wong, K.-T.; Plötzing, T.; Först, M.; Muccini, M. Molecular Host-Guest Energy-Transfer System with an Ultralow Amplified Spontaneous Emission Threshold Employing an Ambipolar Semiconducting Host Matrix. *J. Phys. Chem. B* **2010**, *114*, 120–127.

(10) Weitz, R. T.; Amsharov, K.; Zschieschang, U.; Villas, E. B.; Goswami, D. K.; Burghard, M.; Dosch, H.; Jansen, M.; Kern, K.; Klauk, H. Organic n-Channel Transistors Based on Core-Cyanated Perylene Carboxylic Diimide Derivatives. *J. Am. Chem. Soc.* **2008**, *130*, 4637–4645.

(11) Yan, H.; Zheng, Y.; Blache, R.; Newman, C.; Lu, S.; Woerle, J.; Facchetti, A. Solution Processed Top-Gate n-Channel Transistors and Complementary Circuits on Plastics Operating in Ambient Conditions. *Adv. Mat.* **2008**, *20*, 3393–3398.

(12) Szendrei, K.; Jarzab, D.; Chen, Z.; Facchetti, A.; Loi, M. A. Ambipolar All-Polymer Bulk Heterojunction Field-Effect Transistors. *J. Mater. Chem.* **2010**, *20*, 1317–1321.

(13) Sirringhaus, H. Device Physics of Solution-Processed Organic Field-Effect Transistors. *Adv. Mat.* **2005**, *17*, 2411–2425.

(14) Marcus, R. A. On the Theory of Oxidation-Reduction Reactions Involving Electron Transfer. I. *J. Chem. Phys.* **1956**, *24*, 966–978.

(15) Marcus, R. A. Electron Transfer Reactions in Chemistry. Theory and Experiment. *Rev. Mod. Phys.* **1993**, *65*, 599–610.

(16) Yavuz, I.; Martin, B. N.; Park, J.; Houk, K. N. Theoretical Study of the Molecular Ordering, Paracrystallinity, And Charge Mobilities of Oligomers in Different Crystalline Phases. *J. Am. Chem. Soc.* **2015**, *137*, 2856–2866.

(17) McMahon, D. P.; Troisi, A. Evaluation of the External Reorganization Energy of Polyacenes. *J. Phys. Chem. Lett.* **2010**, *1*, 941–946.

(18) Norton, J. E.; Brédas, J.-L. Polarization Energies in Oligoacene Semiconductor Crystals. *J. Am. Chem. Soc.* **2008**, *130*, 12377–12384.

(19) Lax, M. The Franck-Condon Principle and Its Application to Crystals. *J. Chem. Phys.* **1952**, *20*, 1752–1760.

(20) Kubo, R.; Toyozawa, Y. Application of the Method of Generating Function to Radiative and Non-Radiative Transitions of a Trapped Electron in a Crystal. *Prog. Theor. Phys.* **1955**, *13*, 160–182.

(21) Nan, G.; Yang, X.; Wang, L.; Shuai, Z.; Zhao, Y. Nuclear Tunneling Effects of Charge Transport in Rubrene, Tetracene, and Pentacene. *Phys. Rev. B* **2009**, *79*, 115203.

(22) Borrelli, R.; Peluso, A. The Temperature Dependence of Radiationless Transition Rates from Ab Initio Computations. *Phys. Chem. Chem. Phys.* **2011**, *13*, 4420–4426.

(23) Borrelli, R.; Capobianco, A.; Peluso, A. Generating Function Approach to the Calculation of Spectral Band Shapes of Free-Base Chlorin Including Duschinsky and Herzberg-Teller Effects. *J. Phys. Chem. A* **2012**, *116*, 9934–9940.

(24) Borrelli, R.; Capobianco, A.; Peluso, A. Franck-Condon Factors: Computational Approaches and Recent Developments. *Can. J. Chem.* **2013**, *91*, 495–504.

(25) Borrelli, R.; Peluso, A. Elementary Electron Transfer Reactions: from Basic Concepts to Recent Computational Advances. *WIREs: Comput. Mol. Sci.* **2013**, *3*, 542–559.

(26) Sumi, H.; Kakitani, T. Electron Transfer via a midway molecule as seen in primary processes in photosynthesis; a new process describable as superexchange or sequential in mutually opposite limits. *Chem. Phys. Lett.* **1996**, *252*, 85–93.

(27) Renger, T.; Marcus, R. A. Variable Range Hopping Electron Transfer Through Disordered Bridge States: Application to DNA. *J. Phys. Chem. A* **2003**, *107*, 8404–8419.

(28) Borrelli, R.; Capobianco, A.; Peluso, A. Hole Hopping Rates in Single Strand Oligonucleotides. *Chem. Phys.* **2014**, *440*, 25–30.

(29) Kubo, R. Stochastic Liouville Equations. *J. Math. Phys.* **1963**, *4*, 174–183.

(30) Mukamel, S. *Principles of Nonlinear Optical Spectroscopy*; Oxford University Press: USA, 1995; Chapter 3.

(31) Breuer, F., H.-P.; Petruccione *The Theory of Open Quantum Systems*; Oxford University Press: USA, 2002; Chapter 3.

(32) Kampen, N. V. A cumulant expansion for stochastic linear differential equations. I. *Physica* **1974**, *74*, 215–238.

(33) Izmaylov, A. F.; Mendive–Tapia, D.; Bearpark, M. J.; Robb, M. A.; Tully, J. C.; Frisch, M. J. Nonequilibrium Fermi golden rule for electronic transitions through conical intersections. *J. Chem. Phys.* **2011**, *135*, 234106.

(34) Pereverzev, A.; Bittner, E. R. Time-convolutionless master equation for mesoscopic electron-phonon systems. *J. Chem. Phys.* **2006**, *125*, 104906.

(35) Borrelli, R.; Peluso, A. Quantum Dynamics of Radiationless Electronic Transitions Including Normal Modes Displacements and Duschinsky Rotations: A Second-Order Cumulant Approach. *J. Chem. Theory Comput.* **2015**, *11*, 415–422.

(36) Capobianco, A.; Caruso, T.; Peluso, A. Hole Delocalization over Adenine Tracts in Single Stranded DNA Oligonucleotides. *Phys. Chem. Chem. Phys.* **2015**, *17*, 4750–4756.

(37) Miertiuš, S.; Scrocco, E.; Tomasi, J. Electrostatic Interaction of a Solute with a Continuum. A Direct Utilization of Ab Initio Molecular Potentials for the Prevision of Solvent effects. *Chem. Phys.* **1981**, *55*, 117–129.

(38) D'Avino, G.; Muccioli, L.; Zannoni, C.; Beljonne, D.; Soos, Z. G. Electronic Polarization in Organic Crystals: A Comparative Study of Induced Dipoles and Intramolecular Charge Redistribution Schemes. *J. Chem. Theory Comput.* **2014**, *10*, 4959–4971.

(39) Frisch, M. J.; Trucks, G. W.; Schlegel, H. B.; Scuseria, G. E.; Robb, M. A.; Cheeseman, J. R.; Scalmani, G.; Barone, V.; Mennucci, B.; Petersson, G. A.; Nakatsuji, H.; Caricato, M.; Li, X.; Hratchian, H. P.; Izmaylov, A. F.; Bloino, J.; Zheng, G.; Sonnenberg, J. L.; Hada, M.; Ehara, M.; Toyota, K.; Fukuda, R.; Hasegawa, J.; Ishida, M.; Nakajima, T.; Honda, Y.; Kitao, O.; Nakai, H.; Vreven, T.; Montgomery, J. A., Jr.; Peralta, J. E.; Ogliaro, F.; Bearpark, M.; Heyd, J. J.; Brothers, E.; Kudin, K. N.; Staroverov, V. N.; Kobayashi, R.; Normand, J.; Raghavachari, K.; Rendell, A.; Burant, J. C.; Iyengar, S. S.; Tomasi, J.; Cossi, M.; Rega, N.; Millam, J. M.; Klene, M.; Knox, J. E.; Cross, J. B.; Bakken, V.; Adamo, C.; Jaramillo, J.; Gomperts, R.; Stratmann, R. E.; Yazyev, O.; Austin, A. J.; Cammi, R.; Pomelli, C.; Ochterski, J. W.; Martin, R. L.; Morokuma, K.; Zakrzewski, V. G.; Voth, G. A.; Salvador, P.; Dannenberg, J. J.; Dapprich, S.; Daniels, A. D.; Farkas, Ö.; Foresman, J. B.; Ortiz, J. V.; Cioslowski, J.; Fox, D. J. Gaussian 09 Revision D.01. Gaussian Inc. Wallingford CT 2009.

(40) Borrelli, R.; Peluso, A. MolFC: A program for Franck-Condon integrals calculation. Package available online at `http://www.theochem.unisa.it`.

(41) Borrelli, R.; Peluso, A. The Vibrational Progressions of the N ← V Electronic Transition of Ethylene. A Test Case for the Computation of Franck-Condon Factors of Highly Flexible Photoexcited Molecules. *J. Chem. Phys.* **2006**, *125*, 194308–8.

(42) Borrelli, R.; Peluso, A. Erratum: "The Vibrational Progressions of the N ← V Electronic Transition of Ethylene: A Test Case for the Computation of Franck-Condon Factors of Highly Flexible Photoexcited Molecules". *J. Chem. Phys.* **2013**, *139*, 159902–1.

(43) Peluso, A.; Borrelli, R.; Capobianco, A. Photoelectron Spectrum of Ammonia, a Test Case for the Calculation of Franck–Condon Factors in Molecules Undergoing Large Geometrical Displacements upon Photoionization. *J. Phys. Chem. A* **2009**, *113*, 14831–14837.

(44) Peluso, A.; Borrelli, R.; Capobianco, A. Correction to "Photoelectron Spectrum of Ammonia, a Test Case for the Calculation of Franck-Condon Factors in Molecules Undergoing Large Geometrical Displacements upon Photoionization". *J. Phys. Chem. A* **2013**, *117*, 10985–10985.

(45) Capobianco, A.; Borrelli, R.; Noce, C.; Peluso, A. Franck-Condon Factors in Curvilinear Coordinates: The Photoelectron Spectrum of Ammonia. *Theor. Chem. Acc.* **2012**, *131*, 1181.

(46) Borrelli, R.; Peluso, A. Quantum Dynamics of Electronic Transitions with Gauss-Hermite Wave Packets. *J. Chem. Phys.* **2016**, *144*, 114102.

(47) Park, T. J.; Light, J. C. Unitary quantum time evolution by iterative Lanczos reduction. *J. Chem. Phys.* **1986**, *85*, 5870–5876.

(48) Lubich, C. *From Quantum to Classical Molecular Dynamics: Reduced Models and Numerical Analysis*; European Mathematical Society Publishing House: Zuerich, Switzerland, 2008; Chapter 10.

(49) Bakulin, A. A.; Lovrincic, R.; Yu, X.; Selig, O.; Bakker, H. J.; Rezus, Y. L. A.; Nayak, P. K.; Fonari, A.; Coropceanu, V.; Brédas, J.-L.; Cahen, D. Mode-selective vibrational modulation of charge transport in organic electronic devices. *Nat. Commun.* **2015**, *6*, 7880.

(50) Wen, S.-H.; Li, A.; Song, J.; Deng, W.-Q.; Han, K.-L.; Goddard, W. A. First-Principles Investigation of Anistropic Hole Mobilities in Organic Semiconductors. *J. Phys. Chem. B* **2009**, *113*, 8813–8819.

(51) Schmidt, W. Photoelectron spectra of polynuclear aromatics. V. Correlations with ultraviolet absorption spectra in the catacondensed series. *J. Chem. Phys.* **1977**, *66*, 828–845.

(52) He, Y.; Bussolotti, F.; Xin, Q.; Yang, J.; Kera, S.; Ueno, N.; Duhm, S. Transient Monolayer Structure of Rubrene on Graphite: Impact on Hole–Phonon Coupling. *J. Phys. Chem. C* **2016**, *120*, 14568–14574.

(53) Malagoli, M.; Coropceanu, V.; da Silva Filho, D. A.; Brédas, J. L. A multimode analysis of the gas-phase photoelectron spectra in oligoacenes. *J. Chem. Phys.* **2004**, *120*, 7490–7496.

(54) Borrelli, R.; Di Donato, M.; Peluso, A. Quantum Dynamics of Electron Transfer from Bacteriochlorophyll to Pheophytin in Bacterial Reaction Centers. *J. Chem. Theory Comput.* **2007**, *3*, 673–680.

(55) Borrelli, R.; Capobianco, A.; Landi, A.; Peluso, A. Vibronic Couplings and Coherent Electron Transfer in Bridged Systems. *Phys. Chem. Chem. Phys.* **2015**, *17*, 30937–30945.

(56) Troisi, A.; Orlandi, G. Charge-Transport Regime of Crystalline Organic Semiconductors: Diffusion Limited by Thermal Off-Diagonal Electronic Disorder. *Phys. Rev. Lett.* **2006**, *96*, 086601.

(57) Troisi, A. Prediction of the Absolute Charge Mobility of Molecular Semiconductors: the Case of Rubrene. *Adv. Mat.* **2007**, *19*, 2000–2004.

(58) Ortmann, F.; Bechstedt, F.; Hannewald, K. Charge Transport in Organic Crystals: Theory and Modelling. *physica status solidi (b)* **2011**, *248*, 511–525.

(59) Ren, J.; Vukmirović, N.; Wang, L.-W. Nonadiabatic Molecular Dynamics Simulation for Carrier Transport in a Pentathiophene Butyric Acid Monolayer. *Phys. Rev. B* **2013**, *87*, 205117.

(60) Heck, A.; Kranz, J. J.; Kubar, T.; Elstner, M. Multi-Scale Approach to Non-Adiabatic Charge Transport in High-Mobility Organic Semiconductors. *J. Chem. Theory Comput.* **2015**, *11*, 5068–5082, PMID: 26574305.

(61) Spencer, J.; Gajdos, F.; Blumberger, J. FOB-SH: Fragment orbital-based surface hopping for charge carrier transport in organic and biological molecules and materials. *J. Chem. Phys.* **2016**, *145*, 064102.

(62) Jurchescu, O. D.; Baas, J.; Palstra, T. T. M. Effect of Impurities on the Mobility of Single Crystal Pentacene. *Appl. Phys. Lett.* **2004**, *84*, 3061–3063.

(63) Wang, L. J.; Peng, Q.; Li, Q. K.; Shuai, Z. Roles of Inter- and Intramolecular Vibrations and Band-Hopping Crossover in the Charge Transport in Naphthalene Crystal. *J. Chem. Phys.* **2007**, *127*, 044506.

(64) Sakanoue, T.; Sirringhaus, H. Band-Like Temperature Dependence of Mobility in a Solution-Processed Organic Semiconductor. *Nature Materials* **2010**, *9*, 736–740.

(65) Marumoto, K.; Kuroda, S.-i.; Takenobu, T.; Iwasa, Y. Spatial Extent of Wave Functions of Gate-Induced Hole Carriers in Pentacene Field-Effect Devices as Investigated by Electron Spin Resonance. *Phys. Rev. Lett.* **2006**, *97*, 256603.

(66) Deng, W.; Sun, L.; Huang, J.; Chai, S.; Wen, S.; Han, K. Quantitative Prediction of Charge Mobilities of π-Stacked Systems by First-Principles Simulation. *Nature Protocols* **2015**, *10*, 632–642.

(67) Stehr, V.; Pfister, J.; Fink, R. F.; Engels, B.; Deibel, C. First-Principles Calculations of Anisotropic Charge-Carrier Mobilities in Organic Semiconductor Crystals. *Phys. Rev. B* **2011**, *83*, 155208.

(68) Lee, J. Y.; Roth, S.; Park, Y. W. Anisotropic Field Effect Mobility in Single Crystal Pentacene. *Appl. Phys. Lett.* **2006**, *88*, 252106.

(69) Ling, M.; Reese, C.; Briseno, A. L.; Bao, Z. Non-Destructive Probing of the Anisotropy of Field-Effect Mobility in the Rubrene Single Crystal. *Synth. Met.* **2007**, *157*, 257 – 260.

(70) Xia, Y.; Kalihari, V.; Frisbie, C. D.; Oh, N. K.; Rogers, J. A. Tetracene Air-Gap Single-Crystal Field-Effect Transistors. *Appl. Phys. Lett.* **2007**, *90*, 162106.

(71) Sarker, B. K.; Khondaker, S. I. Lower Activation Energy in Organic Field Effect Transistors with Carbon Nanotube Contacts. *Solid-State Electronics* **2014**, *99*, 55 – 58.

(72) Zhu, M.; Liang, G.; Cui, T.; Varahramyan, K. Temperature and Field Dependent Mobility in Pentacene-Based Thin Film Transistors. *Solid-State Electronics* **2005**, *49*, 884 – 888.

(73) Nelson, S. F.; Lin, Y.-Y.; Gundlach, D. J.; Jackson, T. N. Temperature-Independent Transport in High-Mobility Pentacene Transistors. *Appl. Phys. Lett.* **1998**, *72*, 1854–1856.

(74) Podzorov, V.; Menard, E.; Borissov, A.; Kiryukhin, V.; Rogers, J. A.; Gershenson, M. E. Intrinsic Charge Transport on the Surface of Organic Semiconductors. *Phys. Rev. Lett.* **2004**, *93*, 086602.

(75) Podzorov, V.; Menard, E.; Rogers, J. A.; Gershenson, M. E. Hall Effect in the Accumulation Layers on the Surface of Organic Semiconductors. *Phys. Rev. Lett.* **2005**, *95*, 226601.

Graphical TOC Entry